International Journal of Engineering Research & Technology (IJERT)
ISSN: 2278-0181
Vol. 1 Issue 7, September - 2012

An Electromagnetic Vibrational Energy Harvesting Using Boost and Buck-Boost Converter

M.Rekha
Shri Vishnu Engineering College for Women
Department of Electrical and Electronics
Bhimavaram, India

Mr.K.P.Swaroop
Shri Vishnu Engineering College for Women
Department of Electrical and Electronics
Bhimavaram, India

Abstract

In this paper, Boost and Buck-Boost converters are used for direct AC-DC conversion without using the front-end bridge rectifier as the bridge rectification is inefficient and is not practical for low voltage microgenerators. The proposed converter consists of the above two converters which are connec- ted in parallel and are operated in the positive and negative half cycles respectively. They are operated in the discontinuous mode to minimize the losses as they are significant in the conversion of low voltage ac to the required dc voltage. Analysis of the converters is carried out to obtain the relation between the power and the duty cycle of the converter. A self starting circuit is proposed for independent operation of the converter. Simulation results are presented to validate the proposed converter.

1. Introduction

The recent development of compact and low powered electronic devices has enabled the development of self-powered devices. The traditional use of batteries for such devices is undesirable due to limited shelf life and replacement accessibility. To avoid this, inertial microgenerators are used which harvest vibrations from the ambience and convert into electrical energy [1]-[6], [8]-[16]. Among the different types of inertial microgenerators, electromagnetic microgenerators are used in this paper [5]-[12].

The electromagnetic microgenerators works on the principle of Faraday's law of electromagnetic induction. It consists of a stationary coil and a permanent magnet which is enable to move due to the ambient vibrations from which emf is induced in the coil. The output voltage of these microgenerators is only few millivolts. Most of the electronic devices typically require a dc voltage of 3.3V [11]-[20]. The conventional power converter consists of two stages: a diode bridge rectifier and a standard Buck or Boost converter dc-dc converter. However the bridge rectification is not feasible for low voltage microgenerators and if feasible, the power conversion is very inefficient due to the forward voltage drops in diodes. In order to avoid the problems of two-stage power conversion, direct ac-to-dc power converters are proposed [15], in which the ac output voltage of microgenerators is processed by a single stage boost type converters.

The proposed converter consists of a boost converter in parallel with buck-boost converter which are operated in the positive and negative half cycles respectively. The output dc bus is realized by using a single capacitor. The standard 2-switch H-bridge converter is as shown in the fig. which can be used for the direct ac-dc boost conversion. The waveform of input voltage and the gate drive pulses of the lower switches are as shown in fig. It can be seen that during positive half cycle switch S2 is kept ON for the entire half cycle and the gate pulse to S1 is controlled and during the negative half cycle, the switch S1 is kept ON for the entire half cycle and the gate pulse to S2 is controller. However, there are various disadvantages in these H-bridge converters. Firstly, during charge and discharge of inductors there are always two devices in the conduction path whereas in the proposed converter there is only one switch in the conduction path during the entire half cycle. So, the device conduction losses are reduced by a factor of two in the proposed converter. Second, in the H-bridge topologies, the implementation of control scheme is difficult due to the floating of input voltage source with respect to ground. Third, as the MOSFET switches are designed for forward conduction, they offer higher on–state resistance in the reverse conduction mode.

In this paper, different control schemes and self-starting circuit is presented. Based on the analysis different control schemes has been proposed. A simplified control scheme of using equal inductors is presented for a high voltage step up ratio. In a

practical energy harvesting scenario the gate driver circuit of the MOSFET and controller circuit are

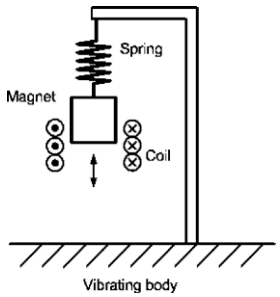

Fig.1.Schematic diagram of a resonance inertial microgenerator

required to be self-starting which are to be powered by the energy harvesting system. In this paper, a self auxiliary circuit is proposed for powering the MOSFET drivers and controller.

The rest of the paper is organized as follows: Section II describes the main circuit topology and the control schemes to control the converter. Section III presents the implementation of the control circuit for the converter and the proposed self-starting circuit. Section IV presents the simulation results .

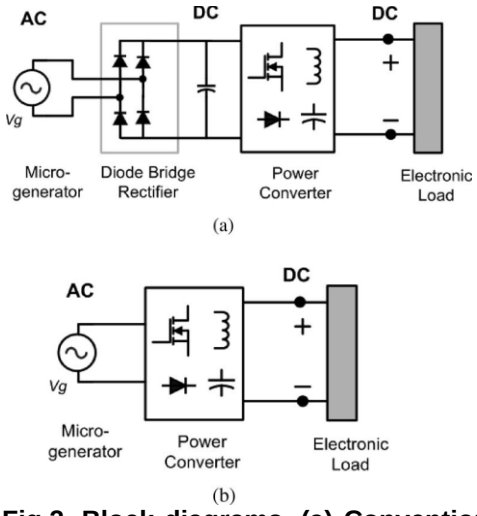

Fig.2. Block diagrams. (a) Conventional two-stage power conversion consisting diode bridge rectifier. (b) Direct ac-to-dc power conversion.

II. Main Circuit Topology

A. Direct AC-DC Converter

The electromagnetic microgenerators typically consist of a moving permanent magnet, linking flux with a stationary coil (see Fig. 1). The variation of the flux linkage induces ac voltage in the coil. In this paper, microgenerator output voltage is modelled as a sinusoidal voltage source. The proposed direct ac-to-dc circuit is as shown in the fig.3. It consists of boost converter in parallel with the buck boost converter. The output capacitor C is charged by the boost converter (comprising of inductor L1, Switch S1, diode D1) during the positive half cycle and by the buck-boost converter (comprising of inductor L2, Switch S2, diode D2) in the negative half cycle respectively. To block the reverse conduction, the forward voltage drop of the body diodes of the MOSFETs is chosen to be higher than the peak of the input ac voltage. Two schottky diodes (D_1 and D_2) with low forward voltage drop are used in the boost and the buck– boost converter circuits for low losses in the diodes.

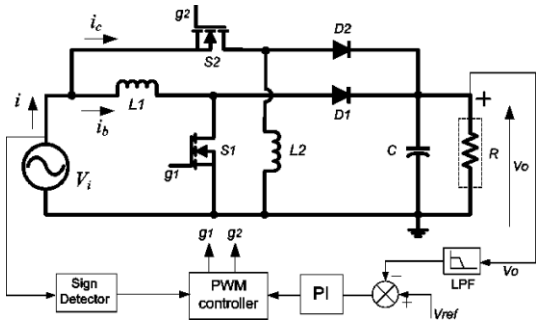

Fig. 3. Proposed direct ac-to-dc converter.

The proposed converter is operated under discontinuous mode of operation (DCM). This reduces the switch turn ON and turn OFF losses. The DCM operation also reduces the diode reverse recovery losses of the boost and buck–boost converter diodes. Furthermore, the DCM operation enables easy implementation of the control scheme. It can be noted that under constant duty cycle DCM operation, the input current is proportional to the input voltage at every switching cycle; therefore, the overall input current will be in-phase with microgenerator output voltage. The converter operation can be divided mainly into four modes. Mode-1 and Mode-2 are for the boost converter operation du- ring the positive half cycle of the input voltage. Under Mode-1, the boost switch S_1 is ON and the current in the boost inductor builds. During Mode-2, the switch is turned OFF and the output capacitor is charged. The other two modes: Mode-3 and Mode-4 are for the buck–boost converter operation during the negative half cycle of the input voltage. Under Mode-3, the buck–boost switch S_2 is ON and current in the buck–boost inductor builds. During Mode-4, the buck–boost switch S_2 is turned OFF and the stored energy of the buck–boost inductor

is discharged to the output capacitor. Detailed discussion of the various modes of operation of the converter is reported in [21].

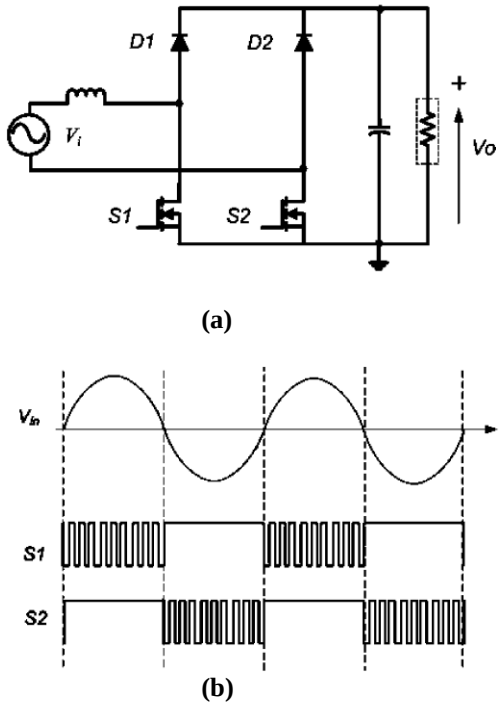

Fig.4. (a) Standard ac–dc boost converter 2-switch H bridge. (b) Input voltage and the gate drive pulsed to the lower switches (S1 and *S*2).

B. Converter Analysis

Consider the input current waveform of the converter as shown in Fig. 5(a). It can be noted that during the boost converter operation, the input current *i* and the boost inductor current (i_{L1}) are equal, but during the buck–boost converter operation, the input current *i* and the current in buck–boost inductor (i_{L2}) are not equal. This is because; in the buck–boost converter the input current becomes zero during the switch turn OFF period (T_{OFF}). Therefore, in a switching cycle, the energy transferred to the output by a buck–boost converter is equal to the energy stored in the inductor, whereas, in the boost converter, the energy transferred to the output is more than the energy stored in the inductor. Hence, for the equal duty cycles, input voltages and inductor values ($L_1 = L_2$), the total powers delivered by the two converters over an input voltage cycle are not equal.

Consider any *k*th switching cycle of the boost and the buck–boost converter as shown in Fig. 5(b), where T_s is the time period of the switching cycle, D_b is the duty cycle of the boost converter, $d_f T_s$ is the boost inductor current fall time (or the diode D_1 conduction time), D_c is the duty cycle of the buck–boost converter, v_i is the input voltage of the generator with amplitude V_p , and V_o is the converter output voltage. Assuming the switching time period (T_s) of the converter is much smaller than the time period of the input ac cycle (T_i), the peak value of the inductor current (i_{Pk}) in the boost converter can be obtained as in (1).

$$i_{Pk} = m_1 D_b T_s = v_{ik} D_b T_s / L_1 \qquad (1)$$

$$where\ v_{ik} = V_p \sin\left(\frac{2\pi k T_s}{T_i}\right).$$

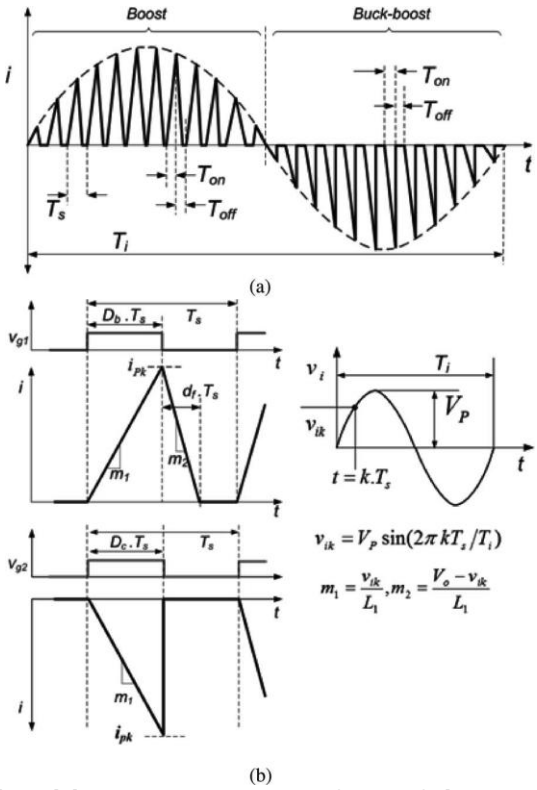

Fig.5.(a) Input current waveform of the converter. (b) Input currents, gate drive signals and input voltage during a switching cycle of boost and buck–boost converter.

After the boost converter switch is turned OFF, the current in inductor starts to fall (see Fig. 5). The slope (m_2) of this current is decided by the voltage across the inductor.

In a *k*th switching cycle, the voltage across the inductor during the inductor current fall time is:

$V_0 - v_{ik}$. Therefore, the inductor current fall time can be found as in (2).

$$d_f\, T_s = \frac{i_{Pk}}{m_2} = \frac{L_1 i_{Pk}}{V_0 - v_{ik}} \qquad (2)$$

During this *k*th switching cycle, the total energy (E_{kb}) transferred from the input of the boost converter can be obtained as in (3)

$$E_{kb} = \frac{v_{ik}\, i_{Pk} (D_b + d_f) T_s}{2}. \qquad (3)$$

The average power supplied in the boost switching cycle is

$$P_{kb} = \frac{E_k}{T_s} = \frac{v_{ik}\, i_{Pk} (D_b + d_f)}{2}. \qquad (4)$$

The number of switching cycles during the time period of one input ac cycle is defined as $N = T_i/T_s$. In the proposed power electronics converter topology, the boost converter is operated for the half time period of the input ac cycle ($T_i/2$). The average input power P_{ib} of the boost converter over this half cycle time period can be obtained as in (5)

$$P_{ib} = \left(\frac{2}{N}\right) \sum_{k=1}^{\frac{N}{2}} P_{kb}$$
$$= \left(\frac{2}{N}\right) \sum_{k=1}^{\frac{N}{2}} \frac{v_{ik}\, i_{Pk} (D_b + d_f)}{2}. \qquad (5)$$

For large *N*, the discrete function in (5) can be treated as a continuous function. The average input power of the boost converter P_{ib} (5) can be obtained by integrating the term in the summation over the half cycle ($T_i/2$) period of the input ac voltage and then taking its mean value. The average power of the boost converter expressed in the integration form can be obtained as in (6)

$$P_{ib} = \frac{2}{T_i} \int_0^{T_i/2} \frac{{D_b}^2 T_s}{2L_1} {V_p}^2 \sin^2\left(\frac{2\pi}{T_i} t\right) \times V_0 \left(V_0 V_p \sin\left(\frac{2\pi}{T_i} t\right)\right)^{-1} dt \qquad (6)$$

Simplifying (6), the average input power for the boost converter P_{ib} is found to be as follows:

$$P_{ib} = \frac{{V_p}^2 {D_b}^2 T_s}{4L_1} \beta$$

Where $\beta = \left(\frac{2}{\pi}\right) \int_0^{\pi} \frac{1}{1-(V_p/V_0)\sin\theta} d\theta$

and $\theta = \frac{2\pi t}{T_i}$. (7)

It can be noted that in (7), β is constant for fixed values of V_p and V_o.

In steady state, the average input power of the converter is equal to the sum of the average output power and the various converter losses. Hence, by defining the converter efficiency as η for a load resistance *R*, the input power and the output power can be balanced as in (8)

$$\frac{{V_p}^2 {D_b}^2 T_s}{4L_1} \beta = \frac{{V_0}^2}{R} \frac{1}{\eta}. \qquad (8)$$

From (8), the duty cycle of the boost converter (D_b) can be obtained as

$$D_b = \frac{2V_0}{V_p} \sqrt{\frac{L_1}{RT_s\eta}} \frac{1}{\beta} \qquad (9)$$

Further, consider the operation of the buck–boost converter; in this case the input power is supplied only during the ON period of the switch S_2 (see Fig. 3). During the OFF period of the switch S_2, the input current is zero [see Fig. 5(a)]. Hence, for any *k*th switching cycle, the average power supplied by the buck–boost converter P_{kc} can be obtained as

$$P_{kc} = \frac{v_{ik}\, i_{Pk} D_c}{2} \qquad (10)$$

Applying similar approach, used earlier for the boost converter, the average power can be expressed in the integration form as

$$P_{ic} = \frac{2}{T_i} \int_0^{T_i/2} \frac{{D_b}^2 T_s}{2L_1} {V_p}^2 \sin^2\left(\frac{2\pi}{T_i} t\right) dt = \frac{{V_p}^2 {D_b}^2 T_s}{4L_1} \qquad (11)$$

The duty cycle D_c can be obtained as in (12)

$$D_c = \frac{2V_0}{V_p} \sqrt{\frac{L_2}{RT_s\eta}}. \qquad (12)$$

C. Control Scheme

Using (9) and (12), the duty cycle of the boost converter Db and the duty cycle of the buck–boost converter D_c can be related as

$$\frac{D_b}{D_c} = \sqrt{\frac{L_1 1}{L_2 \beta}} \qquad (13)$$

Based on (13), two different control schemes can be proposed for the boost and buck–boost-based converter to deliver equal average input power. In scheme 1, the values of the inductors are kept to be equal ($L_2 = L_1$) and the converters are controlled with different duty cycles such that it satisfies the condition: $D_c = D_b\sqrt{\beta}$. In scheme 2, both the boost and the buck–boost converters are controlled with same duty cycle ($D_b = D_c$), whereas the inductor values are chosen to satisfy the condition:$L_1 = \beta L_2$.

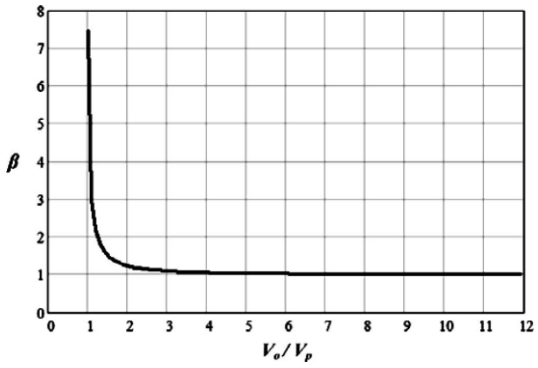

Fig. 6. *β* versus *Vo /Vp* (step-up ratio >1) plot.

In Fig.6, the variable β from (6) is plotted as a function of the step-up ratio (V_o/V_p). It can be seen from this plot that for large values of voltage step-up ratio, β approaches to 1. Hence for higher voltage step-up ratio applications, the boost and the buck–boost converters can be designed with inductors of equal values and they can be controlled with the same duty ratio to successfully deliver the required average power to the output.

This is assistive for the target application of this study, where the very low voltage is stepped up to a much higher dc output voltage. It can be mentioned that the value of β approaches to infinity for $V_o/V_p \rightarrow 1$. Therefore, from (7), the input power for the boost converter may seem to approach infinity as well. But in this case, the duty cycle of the boost converter D_b approaches to zero for $V_o/V_p \rightarrow 1$. Therefore, no power is transferred from the input to the output and the equation remains valid even when $V_o/V_p = 1$.

III. Self-Starting and Control Circuit

In a practical energy-harvesting scenario, the controller and the MOSFET driver circuit of the converter are required to be self-starting and they should be powered by the energy harvesting system. In this study, an auxiliary self-starting circuit, as shown in Fig. 8, is proposed to power the controller and the drivers at the beginning, when the converter starts up.

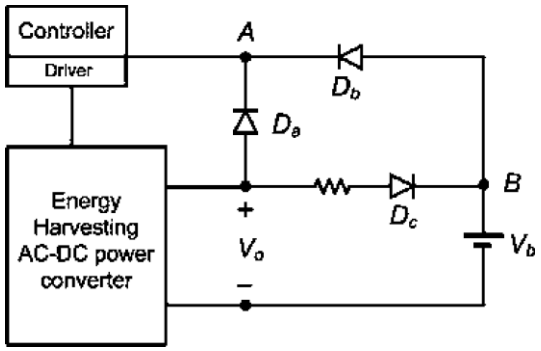

Fig.7. Proposed auxiliary self-starting circuit using a battery.

The proposed self-starting auxiliary circuit utilizes a battery and Schottky diodes for this purpose (see Fig. 8). For the successful operation of this self-starting circuit, the battery nominal voltage V_b should be less than the target output voltage V_o minus the forward voltage drop of a diode V_f, and it should be above the minimum voltage requirements of the controller and driver circuits

$$V_b = V_0 - V_f \quad . \qquad (14)$$

In this study, the target output voltage $V_o = 3.3$ V and forward voltage drop of the diodes V_f=0.22V. A battery with nominal voltage $V_b = 3$ V is selected for the self-starting. At the beginning of the converter operation, when the output voltage V_o is not available, the controller and the driver circuit will be powered by the battery through the Schottky diode D_b. This will allow the converter to charge the output capacitor to the reference voltage. In steady state, when the output voltage has reached the value 3.3 V, the diode D_b would be reverse biased, therefore, the battery will not be powering the controller and the

the driver. At this time, they will be powered from the converter output through the diode D_a . During this condition, the battery will remain under floating condition. It can be noted that only a very small amount of energy is taken from the battery for the startup of the energy harvesting system. Furthermore, the used energy of the battery can be replenished by recharging it from the output of converter through the diode D_c. Therefore, the entire amount of energy used for the converter operation, including the energy used during its starting, is harvested from the ambience.

TABLE I
Converter Circuit Components

Circuit Components	Name	Ratings
Inductor	L_1,L_2	4.7µH
Inductor resistance	R_1	30mΩ
N-channel MOSFET	S_1,S_2	20V,2A
MOSFET on state resistance	R_{ds_on}	150 Ω@ V_{gs}=3V
Schottky Diode	D_1,D_2	23V,1A
Schottky Diode forward voltage	V_f	0.23V
Load resistance	R	200Ω
Capacitor	C	68µF
Capacitor ESR	R_c	30m Ω

IV. Simulation Results

A resonance-based electromagnetic microgenerator, producing 400 mV peak sinusoidal output voltage, with 100-Hz frequency is considered in this study for verification of the proposed converter topology (see Fig. 3). The closed-loop simulation of the converter is carried out based on the control schemes presented in Section II. The reference output voltage (V_{ref}) is considered to be 3.3 V. The energy-harvesting converter is designed for supplying power to a 200-Ω load resistance, hence, supplying about 55 mW of output power. The converter design is carried out based on the analysis and design guidelines, discussed earlier in the Sections II and III. Commercially available MOSFET (Si3900DV from *Vishay*) is selected to realize the switches S_1 and S_2. The forward voltage of the selected MOSFET body diode is about 0.8 V, which is higher than the peak of the input voltage. This inhibits any reverse conduction in the MOSFETs. The nominal duty cycle of the converter is chosen to be 0.7. The inductor is designed to have a standard value of 4.7 μH and commercially available inductor (IHLP-2525CZ from *Vishay*) is used to realize L_1 and L_2 . The diodes, D_1 and D_2 are chosen to be schottky type with low forward voltage (0.23 V, NSR0320 from *ON Semiconductor*). The output capacitor value is 68 μF. Various values for circuit components of the designed converter are presented in Table I. The buck–boost converter duty cycle D_c is calculated from the estimated duty cycle D_b and (13). The input current of the boost converter (see i_b in Fig. 3) and the input current of the buck–boost converter (see i_c in Fig. 3) for load resistance R = 200 Ω is shown in Fig. 9(a) and (b), respectively. The total input current and the microgenerator output voltage (v_i) are shown in Fig. 10 and Fig.8 respectively. It can be seen that the boost converter is operated during the positive half cycle, while the buck–boost converter is operated during negative half cycle of the microgenerator output voltage. The converter output voltage and the duty cycles, estimated by the controller are shown in Fig. 12 and Fig.11, respectively. The output voltage ripple is about ±0.14V, which is ±4.24% of the nominal output voltage. The estimated efficiency of the converter is 63%. For this operating condition, the duty cycle calculated from the analysis of Section II is D_b = 0.71. It can be noted from Fig. 11 that the estimated duty cycle by the controller in the circuit simulation closely matches with value of the duty cycle calculated analytically.

In this study, the output voltage to input voltage peak step-up ratio is: V_o/V_p = 8.25. These corroborate the earlier conclusion from the analysis in Section II (see Fig. 6) that for high step-up ratio, the duty cycles of the converters with same inductor values will be almost equal. To validate this proposed control scheme, further simulations of the converter is carried out for load resistance R = 200 Ω when the boost and buck–boost converter are controlled with same duty ratio. Fig.11, Fig.12 presents the duty cycle and the output voltage of the converter, respectively. To verify the operation of the converter under different load conditions, the load resistance is increased to R = 400 Ω. The output voltage under this load condition is shown in Fig.13. The simulations are carried out with the self-starting circuit (see Fig. 7) . During start-up period of the converter, the power consumed by the control circuit from the battery and the converter is presented in Fig. 14. The battery voltage level and the output voltage

of the converter is also shown in this figure. It can be seen from these plots that at the beginning, when the converter output voltage is building, the power consumed by the control circuit is only supplied by the battery. At point A, as shown in Fig. 14, the converter output voltage becomes higher than the battery voltage. From this point onwards, the power consumed by the control circuit is supplied by the converter, and the power draw from the battery becomes zero (see Fig. 14).). It can be found that the start-up time taken by the converter is about 4.6 ms. This is less than the half cycle period of the input ac voltage (100 Hz). Further, it can be obtained that the average power consumed by the control circuit is about 2.2 mW. Further, the ouput dc voltage(3.3V) is converted in to ac using inverter which is connected to the RL load and the resulting waveforms are shown in the fig.15.

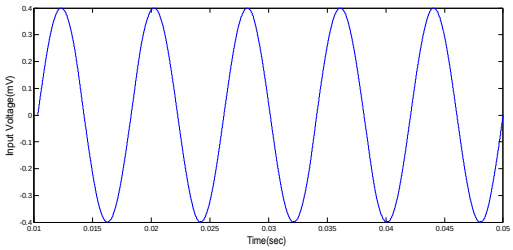

Fig.8.Input voltage

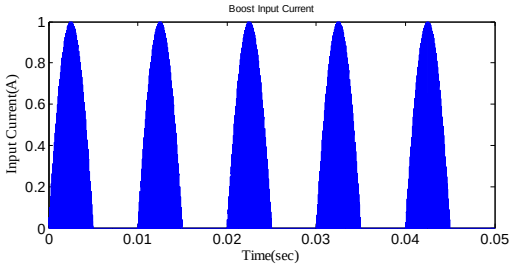

(a)

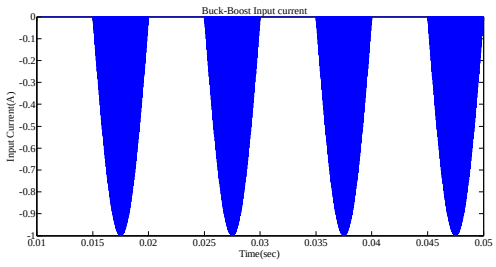

(b)

Fig.9 (a) Boost Input Current, (b) Buck-Boost Input Current

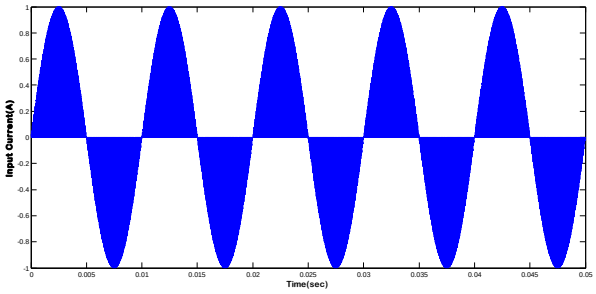

Fig.10.Input Current

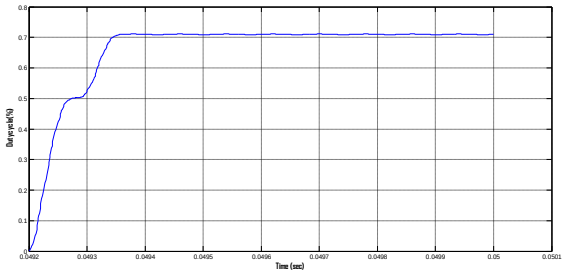

Fig.11.Duty Cycle for R=200Ω

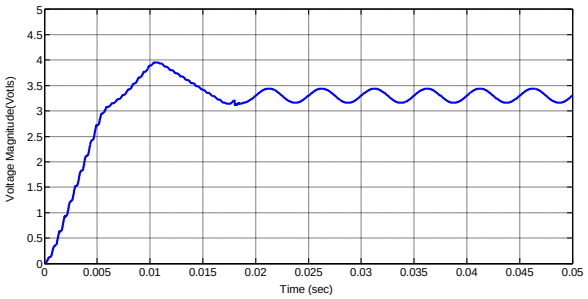

Fig.12. Output voltage for R=200Ω

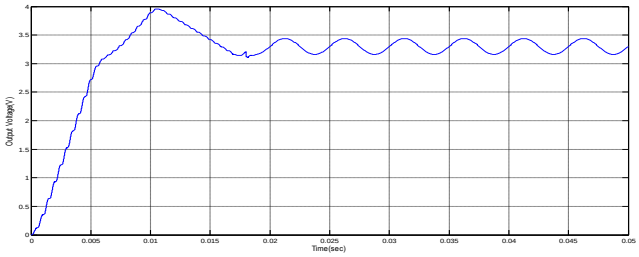

Fig.13. Output voltage for R=400Ω

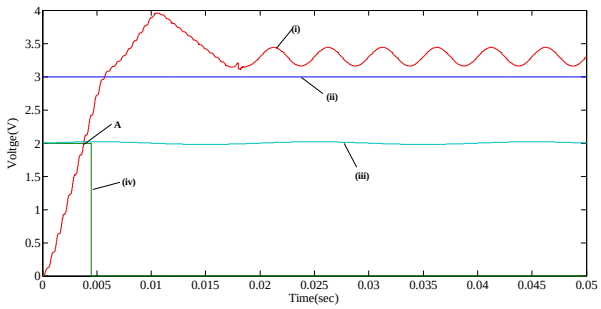

Fig.14. Power and voltages during self start-up. Curves (iv), (iii), (ii), and (i) show the power supplied by the battery, power draw from the converter output, battery voltage, and converter output voltage, respectively.

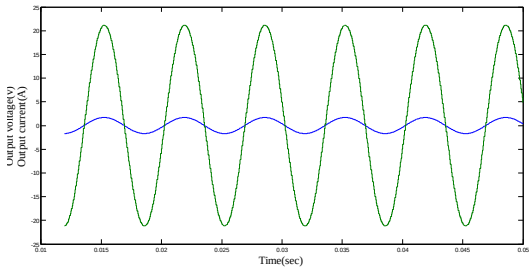

(a)

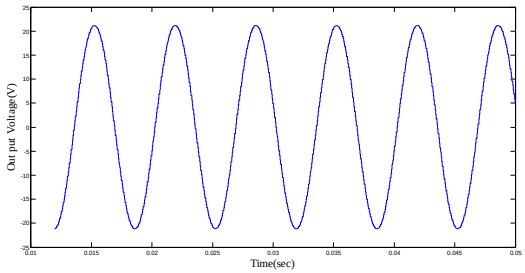

(b)

Fig.15 (a) The generated output voltage and current from the inverter which are in phase, (b)out put voltage

V. Conclusion

The presented direct ac-to-dc low voltage energy harvesting converter avoids the conventional bridge rectification and achieves higher efficiency. The proposed converter consists of a boost converter in parallel with a buck–boost converter The negative gain of the buck–boost converter is utilized to boost the voltage of the negative half cycle of the microgenerator to positive dc voltage. Analysis of the converter for direct ac-to- dc power conversion is carried out and the relations between various converter circuit parameters and control parameters are obtained. Based on the analysis, a simplified control scheme is proposed for high-voltage step-up application. A self-startup circuit, using a battery only during the beginning of the converter operation, is proposed for the energy-harvesting converter. Operation and the implementation of the self-startup circuit and the control circuit of the converter are presented in details. Based on the analysis and the design guidelines, a prototype of the converter is developed. The proposed control scheme with the self-startup circuit is implemented and the converter is successfully operated to directly step-up the low ac voltage to a high dc voltage. The loss components of the converter are estimated. The measured efficiency of the converter is 61% , which is higher than the reported converters.

REFERENCES

[1] J. A. Paradiso and T. Starner, "Energy scavenging for mobile and wireless electronics," *IEEE Pervasive Comput.*, vol. 4, no. 1, pp. 18–27, Jan./Mar.2005.

[2] S. Meninger, J. O. Mur-Miranda, R. Amirtharajah, A. P. Chandrakasan,and J. H. Lang, "Vibration-to-electric energy conversion," *IEEE Trans.Very Large Scale Integr. Syst.*, vol. 9, no. 1, pp. 64–76, Feb. 2001.

[3] M. El-Hami, P. Glynne-Jones, N. M. White, M. Hill, S. Beeby, E. James, A. D. Brown, and J. N. Ross, "Design and fabrication of a new vibration based electromechanical power generator," *Sens. Actuators A: Phys.*,vol. 92, pp. 335–342, 2001.

[4] T. M. Thul, S. Dwari, R. D. Lorenz, and L. Parsa, "Energy harvesting and efficient power generation from human activities," in *Proc. Center Power Electron. Syst. (CPES) Semin.*, Apr. 2007, pp. 452–456.

[5] N. G. Stephen, "On energy harvesting from ambient vibration," *J. Sound Vibrations*, vol. 293, pp. 409–425, 2006.

[6] J. R. Amirtharajah and A. P. Chandrakasan, "Self-powered signal processing using vibration-based power generation," *IEEE J. Solid-State Circuits*, vol. 33, no. 5, pp. 687–695, May 1998.

[7] B. H. Stark, P. D. Mitcheson, M. Peng, T. C. Green, E. Yeatman, and A. S. Holmes, "Converter circuit design, semiconductor device selection and analysis of parasitics for micro power electrostatic generators," *IEEE Trans. Power Electron.*, vol. 21, no. 1, pp. 27–37, Jan. 2006.

[8] C. B. Williams and R. B. Yates, "Analysis of a micro-electric generator for microsystems," in *Proc. Int. Conf. Solid-State Sens. Actuators*, 1995, pp. 369–372.

[9] P.D.Mitcheson, T. C. Green, E.M.Yeatman, and A. S. Holmes, "Architectures for vibration-driven micro power generators," *J. Microelectromech.Syst.*, vol. 13, no. 3, pp. 429–440, Jun. 2004.

[10] S. Xu, K. D. T. Ngo, T. Nishida, G. B. Chung, and A. Sharma, "Low frequency pulsed resonant converter for

energy harvesting," *IEEE Trans.Power Electron.*, vol. 22, no. 1, pp. 63–68, Jan. 2007.
[11] J. Elmes, V. Gaydarzhiev, A. Mensah, K. Rustom, J. Shen, and I. Batarseh,"Maximum energy harvesting control for oscillating energy harvesting systems," in *Proc. IEEE Power Electron. Spec. Conf.*, Jun. 2007, pp. 2792– 2798.
[12] S. P. Beeby, R. N. Torah, M. J. Tudor, P. Glynne-Jones, T. O'Donnell, C. R.Saha, and S. Roy, "Microelectromagnetic generator for vibration energy harvesting," *J. Micromech. Microeng.*, vol. 17, pp. 1257–1265, 2007.
[13] B. H. Stark, P. D. Mitcheson, M. Peng, T. C. Green, E. Yeatman, and A. S. Holmes, "Converter circuit design, semiconductor device selection and analysis of parasitics for micro power electrostatic generators," *IEEE Trans. Power Electron.*, vol. 21, no. 1, pp. 27–37, Jan. 2006.
[14] T. Paing, J. Shin, R. Zane, and Z. Popovic, "Resistor emulation approach to low-power RF energy harvesting," *IEEE Trans. Power Electron.*, vol. 23,no. 3, pp. 1494–1501, May 2008.
[15] E. Lefeuvre, D. Audigier, C. Richard, and D. Guyomar, "Buck-boost converter for sensorless power optimization of piezoelectric energy harvester,"*IEEE Trans. Power Electron.*, vol. 22, no. 5, pp. 2018–2025, Sep.2007.
[16] X. Cao,W.-J. Chiang,Y.-C.King, andY.-K. Lee, "Electromagnetic energy harvesting circuit with feedforward and feedback DC–DC PWM boost converter for vibration power generator system," *IEEE Trans. Power Electron.*, vol. 22, no. 2, pp. 679–685, Mar. 2007.
[17] G. K. Ottman, H. F. Hofmann, and G. A. Lesieutre, "Optimized piezoelectric energy harvesting circuit using step-down converter in discontinuous conduction mode," *IEEE Trans. Power Electron.*, vol. 18, no. 2, pp. 696–703, Mar. 2003.
[18] G. K. Ottman, H. F. Hofmann, A. C. Bhatt, and G. A. Lesieutre, "Adaptive piezoelectric energy harvesting circuit for wireless remote power supply,"*IEEE Trans. Power Electron.*, vol. 17, no. 5, pp. 669–676, Sep. 2002.
[19] M. Ferrari, V. Ferrari, D. Marioli, and A. Taroni, "Modeling, fabrication and performance measurements of a piezoelectric energy converter for power harvesting in autonomous microsystems," *IEEE Trans. Instrum.Meas.*, vol. 55, no. 6, pp. 2096–2101, Dec. 2006.
[20] P. D. Mitcheson, T. C. Green, E. M. Yeatman, and A. S. Holmes, "Power processing circuits for electromagnetic, electrostatic and piezoelectric inertial energy scavengers," *Microsyst. Technol.*, vol. 13, pp. 1629–1635,May 2007.
[21] S. Dwari, R. Dayal, and L. Parsa, "A novel direct AC/DC converter for efficient low voltage energy harvesting," in *Proc. IEEE Ind. Electron. Soc.Annu. Conf.*, Nov. 2008, pp. 484–488.
[22] A. Richelli, L. Colalongo, S. Tonoli, and Z.M. Kov´acs-Vajna, "A 0.2−1.2 VDC/DC boost converter for power harvesting applications," *IEEE Trans,Power Electron.*, vol. 24, no. 6, pp. 1541–1546, Jun. 2009.